ELSEVIER

Polymer 42 (2001) 5661–5667

polymer

www.elsevier.nl/locate/polymer

Changes in structural and mechanical behaviour of PVDF with processing and thermomechanical treatments. 1. Change in structure

Badr-Eddine El Mohajir*, Nicole Heymans

Université Libre de Bruxelles, Physique des Matériaux de Synthèse CP 194/08, 84 av. A Buyl-1050 Brussels, Belgium

Received 19 October 1999; received in revised form 15 January 2001; accepted 17 January 2001

Abstract

The present work focuses on the effects of thermomechanical history on the structure and mechanical behaviour of PVDF. In the first part of our investigation differential scanning calorimetry (DSC) and dynamic mechanical analysis (DMA) are used to follow the evolution of the structure of PVDF after different annealing treatments or deformation. Processing has a significant impact on the quantities of the amorphous and crystalline phases and their interphase. Subsequent annealing affects these phases in a different proportion. This influence depends on the position of the annealing temperature in comparison with the upper glass transition temperature of PVDF. Deformation induces conformational change in the injection moulded samples. Thus, the α conformation is transformed to the β conformation. The β conformation also has a noticeable influence on the mechanical behaviour of the material, which will be discussed in the second part of our study. © 2001 Elsevier Science Ltd. All rights reserved.

Keywords: PVDF; Thermomechanical history; Processing technique

1. Introduction

PVDF has remarkable chemical, electrical and mechanical properties [1,2]. The discovery of its piezo and pyro-electrical properties had motivated most of the work on it [3,4].

PVDF is a semi-crystalline polymer presenting a complex structure with 4 possible conformations [5–7]. The α (TG^+TG^-) conformation is the most common. The β conformation, which is responsible for the piezo and the pyro-electrical properties, has a TTT conformation. The γ form has a GTTT conformation while δ corresponds to the polar form of α.

The conditions under which a specific conformation can be obtained depend strongly on the processing, thermal or mechanical treatments that the polymer undergoes. The α conformation may be obtained after supercooling or a quench [8]. The β conformation can be obtained by stretching the polymer with α conformation. Several authors investigated the optimal conditions for this conversion [9–11].

Gregorio et al. [12] studied the position of the melting temperature of each conformation. They find that the melting of γ conformation occurs at temperatures higher than the α or β conformation. However, the melting temperatures vary considerably with the conditions of polymerisation, which influences the average molecular weight, and the processing parameters, such as pressure, as observed by Matsushige and al [13].

On melting, PVDF can therefore present several peaks linked to the presence of several conformations, or crystallites of different sizes [8,12].

In addition to melting, PVDF presents also several transitions. The principal ones are the lower glass transition, around (233 K), corresponding to the amorphous phase, and the upper glass transition, corresponding to the amorphous-crystalline interphase (a–c interphase), between 303 and 333 K. Other transitions above 333 K might correspond to pre-melting phenomena. Their appearance at high temperatures depends on treatment or processing [14].

The aim of the first part of our work is to analyse the structural transformations in PVDF after different thermomechanical treatments. The second part will concern the analysis of the evolution of its mechanical behaviour after these treatments to determine the influence of the structural transformation.

These treatments consist initially of the processing technique, then on annealing at various temperatures as well as stretching samples in tension.

* Corresponding author. Tel.: +32-2-6502759; fax: +32-2-6502766.

PII: S0032-3861(01)00064-7

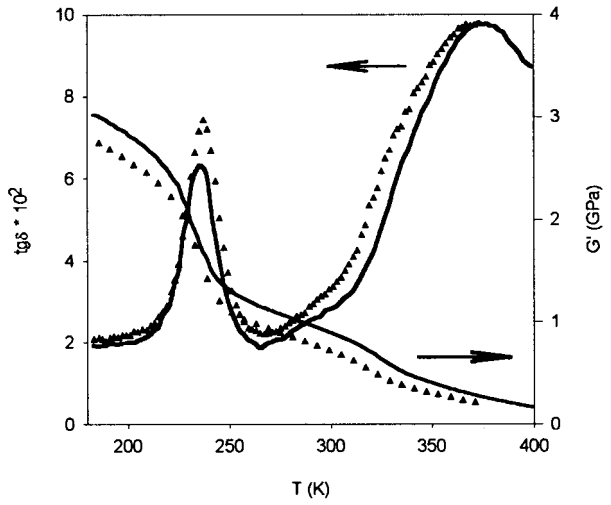

Fig. 1. Dynamic measurements, loss tangent and storage modulus, of IM (triangles) and CM (full line) as-delivered samples.

2. Experimental

2.1. Sample preparation

The samples, provided by Solvay NOH, are commercialised as Solef. The α conformation alone is present.

Tensile samples, ISO 1B, are prepared by injection moulding (IM) or by cutting out of pressed plates (CM). Cross-sectional dimensions are approximately (2×9.94) and (2.11×11.6) mm^2, respectively. The length of the gauge section is 60 mm.

A set of injection-moulded samples (IMB) is characterised by a lower cross-section, which does not exceed 1.98×9.88 mm^2.

The samples used for dynamic measurement are parallelipipedic, with a dimension of approximately $36 \times 5 \times 1$ mm^3.

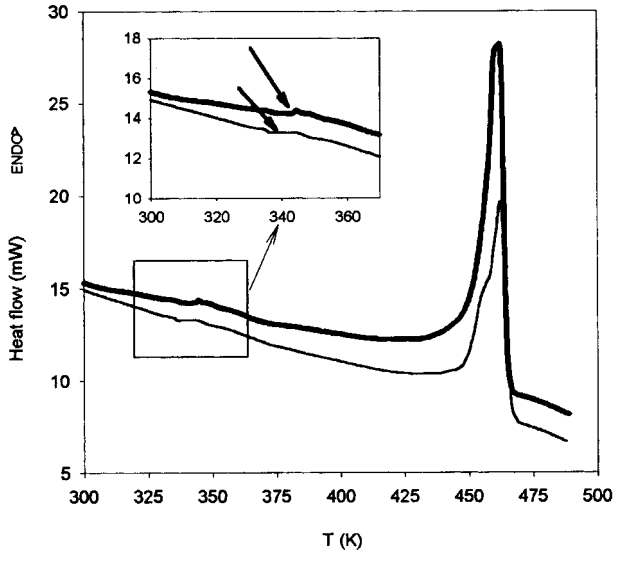

Fig. 2. DSC measurements of IM (sharp line) and CM (thick line) as-delivered samples.

All treatments are preceded by a standardisation treatment, i.e. by annealing at 423 K for approximately one hour. At this annealing temperature most of the thermomechanical history of samples is erased without altering their shape. Annealing was then carried out at various temperatures, chosen for their position in relation to the upper glass transition: 296, 313 and 353 K. The annealing duration is 1 or 10 days.

Samples were deformed at room temperature in an Instron stretching machine. They were left for 1hour at room temperature after the treatment and were then stretched at 0.1 or 0.01 cm/min until break. DSC samples were taken from the stretched part near the break and in the non-deformed part to determine the effect of stretching on crystalline and amorphous phases and their interphase.

3. Measurements

3.1. Dynamic measurements

These measurements were taken during a temperature sweep between 183 and 400 K at 1 Hz frequency in a Metravib torsional pendulum, and at a heating rate of 1 K/min. The samples were removed from the annealing oven, placed in the pendulum and cooled to 183 K with liquid nitrogen. They were then kept at this temperature for approximately 30 min before taking the measurements.

The temperature position for the lower and upper glass transitions and their amplitude were determined from the storage modulus. In addition, we look at the loss tangent, which by analysing the peak surface of the lower glass transition, informs us about the amorphous phase quantity.

3.2. Calorimetric measurements

These were performed on a Perkin–Elmer DSC-2C. Measurements were taken on samples of approximately 15 mg, cut perpendicularly to the surface. Other measurements were taken on samples cut parallel to the surface to detect the difference between the core and the skin of the samples. The heating rate was 10 K/min. These measurements allow the evolution of the crystalline phase quantity and in a lesser proportion the evolution of the a–c interphase, to be followed.

4. Experimental results

4.1. Effects of the processing technique

In the curve of the loss tangent Tgδ (Fig. 1), the peak corresponding to the lower glass transition, situated around 234 K, indicates that there is more amorphous phase in IM than CM. We observe clearly that the area corresponding to

Table 1
Melting temperature (T_{max}) and heat of melting (H) for stretched and non-stretched treated samples

Tensile sample	Injected (IM)				Pressed (CM)			
Fraction of sample →	Non-deformed		Deformed		Non-deformed		Deformed	
Treatment ↓	Tmax K	H cal/g	Tmax (K)	H cal/g	Tmax K	H cal/g	Tmax (K)	H (cal/g)
As-Delivered	449.8	13.64	450.78 466.1[a]	14.31 0.18[a]	448.9	14.73	444.94	14.78
Standardised	450.39	14.69	446.24 465.36[a]	14.56 0.22[a]	449.81	15.4	447.76	15.33
+ 10 days 23°C	449.24	14.92	447.29 464.33[a]	15.02 0.21[a]	448.98	15.44	444.12	15.49
+ 10 days 40°C	447.85	13.72	446.25 464.68[a]	14.8 0.21[a]	449.23	15.82	449.5	15.84
+ 10 days 80°C	449.3	14.81	447.3 464.43[a]	15.2 0.23[a]	448.78	16.14	449.03	16.13

[a] Correspond to temperature and heat melting of peak at 465 K (β conformation).

that peak is higher for IM. The peak temperature is similar for all the different samples. However, the temperature of the upper glass transition varies considerably with the processing technique; this can be seen clearly on the storage modulus curves but not from the DSC measurements. We have thus a Tg_U equal to ~323 and 318 K for CM and IM, respectively. The DSC trace (Fig. 2) gives a temperature of ~332 K in the two cases, but with a larger transition for CM.

Concerning the crystalline phase, the melting heat is higher for the CM (Table 1). Their crystallinity is therefore higher than for IM. Also, a multiple peak is present only for IM melting (Fig. 2). We also notice for IMB, the appearance of a small peak, above the main melting peak, at 465 K. This peak is localised mainly at the surface of the IMB samples as shown in (Fig. 2, insert). Indeed, the peak is absent in the DSC trace of the sample core.

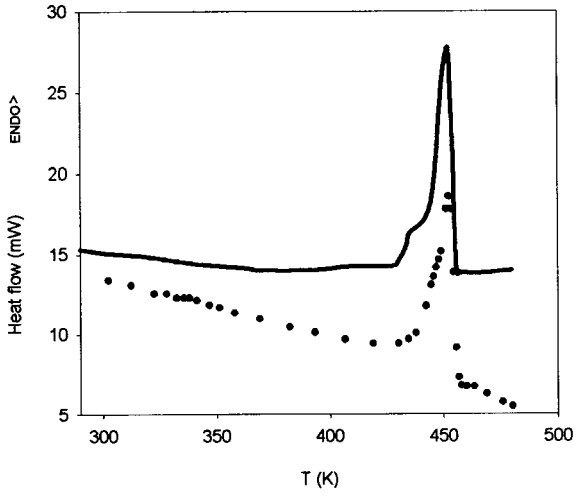

Fig. 3. DSC measurements of IM as-delivered sample (circles) and after standardisation (full line).

4.2. Effects of standardisation annealing

This annealing is carried out to delete the thermo-mechanical history of the sample before any additional treatment. A part of this history is recorded in the crystalline phase, and can be deleted only by annealing at a temperature above the melting temperature (~450 K).

However, the standardisation annealing modifies the crystalline structure and erases the effects of all annealing and ageing undertaken at lower temperatures. In the DSC trace of IM shown in Fig. 3, we notice the appearance of a shoulder just before the main melting peak, which becomes narrower, as well as a wide tail before the shoulder. In the case of the samples with completely different thermo-mechanical history, their mechanical behaviour is similar after this annealing [15]. A change in crystallinity is also observed. Indeed, we notice an increase after standardisation compared to the as-delivered sample, thus the melting heat increases from 13.6 to 14.7 cal/g for the IM. The transition corresponding to the a–c interphase disappears or weakens.

In the dynamic measurements (Fig. 4), a false peak appears in the loss tangent curve with characteristics similar to those of an annealing peak [16,17], in the area of the upper glass transition. The false peak appears after cooling and can be lessened by annealing in this range of temperature. This affects the storage modulus curve and makes therefore the observation of any transition in this temperature range difficult.

In the lower glass transition, we distinguish clearly an increase in the area of the loss tangent peak after standardisation (Fig. 4), indicating an increase of the amorphous phase quantity.

4.3. Effects of post-standardisation thermal treatments

As mentioned previously, this treatment consists in

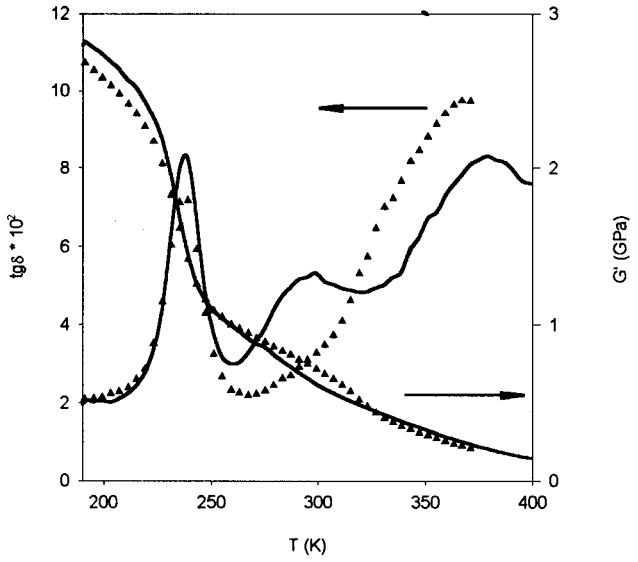

Fig. 4. Dynamic measurements, loss tangent and storage modulus, of IM as-delivered sample (triangles) and after standardisation (full line).

annealing during 1 or 10 days at a temperature of 296, 313 and 353 K.

Annealing at 296 and 313 K has similar effects. Their corresponding dynamic measurements (Fig. 5) show a larger decrease of the amorphous phase than after annealing at 353 K. The latter is similar to standardisation in its effects.

Also, after annealing at 296 and 313 K, more a–c interphase, which was invisible after standardisation, reappears. This is shown by the transition in the real modulus curve around 325 K. Furthermore, the upper glass transition

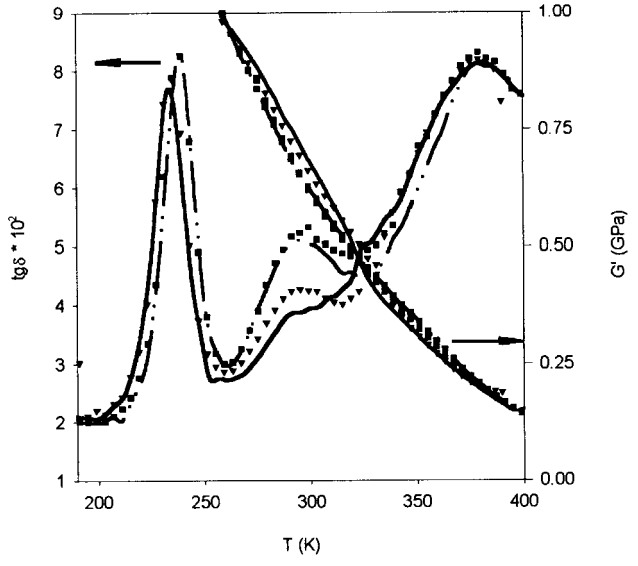

Fig. 5. Dynamic measurements, loss tangent and storage modulus, of IM sample standardised (square) and annealed 1 day at, 353 K (dash-dot-dot), 313 K (triangles) and at 296 K (full line).

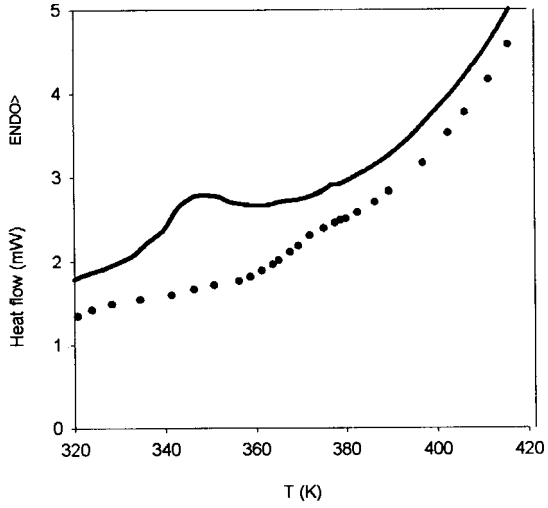

Fig. 6. DSC measurements of IM standardised samples annealed for 1 day at 313 K (full line) and 353 K (circles).

temperature Tg_U is higher after annealing at 353 K, but the amplitude is larger after annealing at 296 K. The rate of change of the properties is greater if the treatment temperature is higher. Thus, saturation is reached sooner at 353 than at 296 K. More details will be given on these results in our paper concerning the effects on the mechanical properties [15]. The DSC measurements confirm the dynamic results. Indeed, an upper glass transition appears after annealing at 296 and 313 K, as well as their difference in the temperature position (Fig. 6). After annealing at 296 K, the Tg_U is equal to 312 K, while equal to 335 K after annealing at 313 K.

Concerning crystallinity (Table 1), no evolution for IM with annealing is observed. For CM samples, the crystallinity is higher after annealing at 353, followed by 313, then by 296 K and last by the standardisation annealing.

4.4. Stretching effects:

The comparison of the samples cut from the region close to the break with non-deformed samples allows us to observe the effects of plastic deformation on the structure of the polymer. These effects are different for IM and CM samples. We observe for IM samples that the deformation is homogeneous and accompanied by a slight increase in the quantity of the crystalline phase (Table 1). We also observe the appearance of a new melting peak around 465 K (Fig. 7), above the ordinary melting peak of α conformation. This peak is attributed to the β conformation.

For CM samples, no increase in crystallinity is seen, nor appearance of any new peak. However, we observe a neck propagating along the sample before rupture. Necking is also observed in IMB samples.

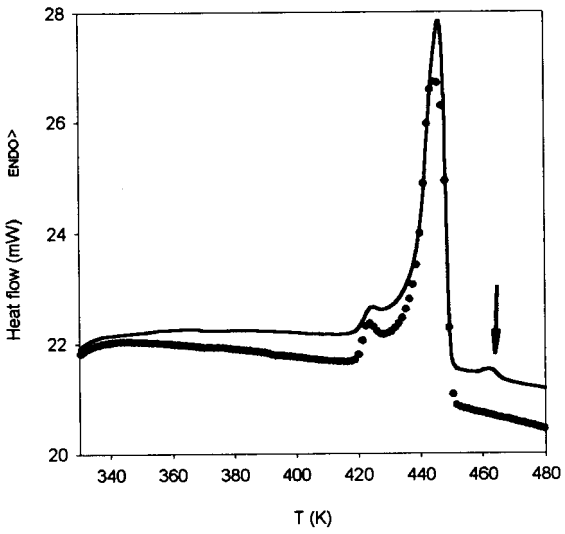

Fig. 7. DSC measurements of IM standardised samples non-stretched (circles) and stretched at room temperature (full line).

5. Discussion

The influence of the processing technique on the phase quantities in the polymer is obvious. Injection moulding enables the appearance of more amorphous phase while compression moulding leads to more crystalline phase. This is due to the differences in the principle of the two techniques. During injection moulding, the sample is cooled rapidly in the mould, which leads to incomplete crystallisation with formation of small size crystallites, and thus to more amorphous phase. In contrast, pressed samples are cooled more slowly from the melt towards room temperature, allowing more crystallisation and formation of larger crystals.

The a–c interphase depends on the crystalline phase area; smaller crystals having greater area lead to more interphase; that should be the case for IM samples. However, as crystallinity is lower in IM compared to CM samples, more interphase is obtained for CM. The dynamic measurements show this behaviour better, as its equivalent heating rate is 10 times smaller than DSC.

The form of the melting peak of IM samples is more complex than CM samples. We should keep in mind that the DSC samples are cut perpendicularly to the surface so different crystalline sizes are present in IM samples [11]. Thus the sample surface cools more rapidly and is submitted to higher shear stresses during injection than the sample core. Therefore, the crystallite size varies from the surface to the core, and so does the melting peak temperature. For the CM samples, no shearing exists and there is no contact with a cold surface, which decreases the effects of temperature heterogeneity in comparison with IM samples.

The crystalline structure of the polymer depends strongly on the conditions under which it is formed. A high or moderate cooling rate generally produces the α conformation [12]. The latter can be transformed to the β conformation by stretching. This conversion is strongly influenced by the stretching temperature; a maximum is obtained with a temperature around 353 K [9,10]. The β conformation is also observed in samples injection moulded at higher injection rates; as a result, a melting peak appears in the DSC trace around 456 K [11]. Gregorio et al. [12], when isolating each of the two conformations observed that the melting temperature for both of them coincides around 440 K, with a broader melting peak for the β conformation. However, the melting peak of the γ conformation is also situated around 456 K [12]. Therefore, the melting temperature varies considerably with the conditions of polymerisation, which control the average molecular weight and the processing parameters such as pressure. Matsushige et al. [13]studied the effects of pressure on PVDF crystallisation. They observed an increase with pressure of the melting temperature of the α conformation, which is transformed to the β conforation at high pressure. The melting temperature of the α conformation is around 449 K if crystallisation occurs under atmospheric pressure, but can reach 573 K if the pressure exceeds 390 MPa. For the β conformation, the melting temperature varies between 463 and 573 K for the same pressure range.

For the IMB samples, the peak situated at 465 K linked to the β conformation can be due to a higher injection rate or to higher pressure. In addition, the lower thickness of those samples induces an imperfect contact with the mould surface. The sample skin is thus maintained under constraint at high temperature for longer leading to the conversion of the α conformation to β as indicated on Fig. 8a,b illustrates the case of γ conversion and absence of those conversion mechanism in our study which reinforce the hypothesis that the peak at 463 K correspond to β conformation.

The standardisation annealing temperature (423 K) is clearly above the Tg_L (~233 K) and Tg_U (~327 K). At this temperature, the amorphous phase and the a–c interphase are in equilibrium, and any effects of annealing at lower temperature are suppressed. However, those occurring at higher temperature, such as processing, remain. The crystalline quantity in CM samples is thus maintained higher compared to IM samples even after standardisation (Table 1). Therefore, only samples obtained by the same processing technique are in the same state after standardisation.

At 423 K, the polymer is still able to crystallise, that explains the appearance of the shoulder before the melting peak. Indeed, narrowing of the melting peak (Fig. 3) implies recrystallisation of imperfect crystallites. The partial crystallisation of the a–c interphase increases the crystalline fraction (Table 1) and suppresses the interphase transition in the DSC trace.

The amorphous phase fraction also increases at the expense of the a–c interphase (Fig. 4). After the standardisation annealing, the sample is cooled to annealing temperature 296, 313 and 353 K with different cooling rates. The latter process has more pronounced impact on the CM

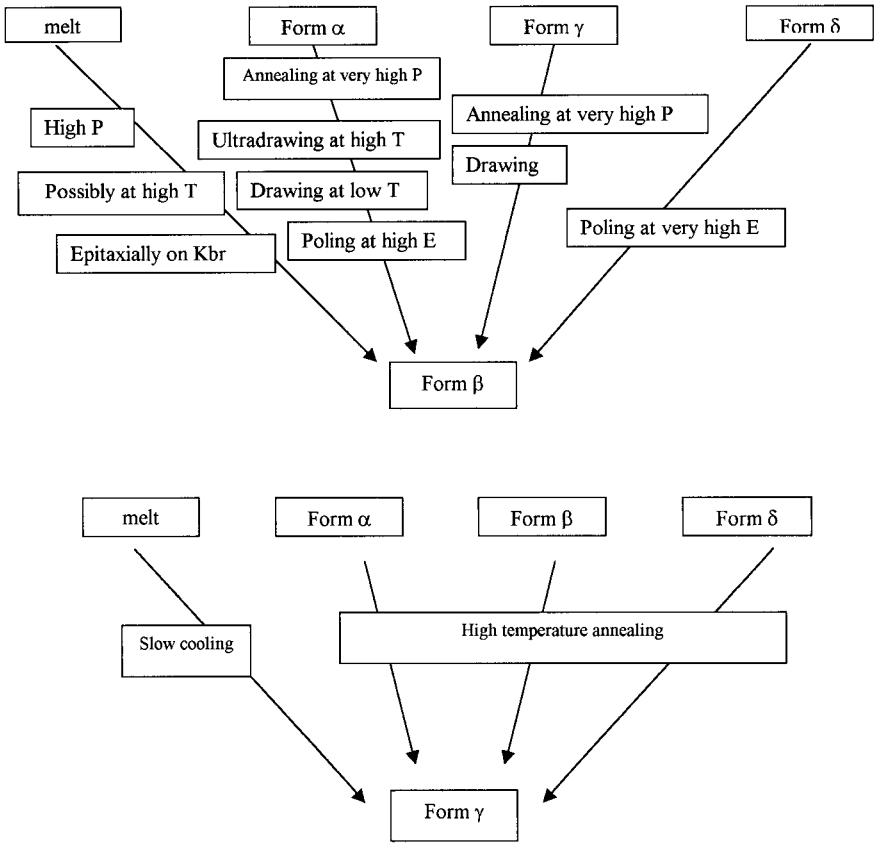

Fig. 8. Transitions from different conformations of PVDF to β and γ conformations [5].

crystallinity (Table 1). The increased crystallinity in 353 K annealed samples corresponds to a lower cooling rate prior to annealing. In contrast, lower crystallinity is obtained in samples annealed at 296 K due to the high cooling rate, as well as after the standardisation because samples are cooled to room temperature before the DSC trace is taken.

For the 296 and 313 K annealing, we note a weak decrease of the amorphous quantity and reappearance of a–c interphase. This suggests that the latter forms at the expense of the first, insofar as these annealing temperatures are below Tg_U. The 353 K annealing does not enable the appearance of the interphase, as the temperature is above Tg_U (Fig. 6).

The increase of crystallinity after IM stretching at room temperature results mainly from the appearance of the β conformation, which implies higher orientation of the crystalline phase. However, it remains low in quantity due to the stretching temperature and at the same time to the thickness of the sample. The formation of the β conformation is optimal in the thin films with stretching temperature around 353 K [10]. Fig. 8a indicates the different routes which allows generation of the β conformation from the melt or from other PVDF conformations.

6. Conclusions and perspectives

DSC and dynamic measurements allow us the observation and the study of the effects of thermomechanical history on PVDF structure. The processing technique influences the structure on all scales, from crystalline to the amorphous phase as well as through their interphase. Indeed, we observe higher crystallinity in CM than IM due to the low cooling rate and to the absence of shear. The impact of subsequent annealing depends on the position of the annealing temperature in comparison to Tg_U. A temperature below Tg_U affects the interphase more, while a higher temperature affects the crystalline phase. The stretching effect is also significant. We clearly see the development of the β conformation from the α conformation for the IM. Changes in crystallinity of CM samples annealed at 353 K or below are attributed to differences in cooling rate prior to annealing rather than to the annealing treatment itself. We will show in the second part of our work the influence of all these structural changes on the mechanical behaviour of PVDF.

Acknowledgements

The authors thank Solvay NOH Belgium for their material support. B.-E. El Mohajir is grateful for financial support from “Fondation Universitaire David et Alice Van Buuren” during the course of this work.

References

[1] Sperati Carleton A. Fluoropolymers, Poly(vinylidene Fluoride) (PVDF). In: Rubin Irvin I, editor. Handbook of plastic materials and technology. New York: Wiley/Interscience, 1990. p. 131–6.

[2] Sperati Carleton A. Physical constants of fluoropolymers. In: Brandrup J, Immergut EH, editors. Polymer handbook, 3rd ed. New York: Wiley/Interscience, 1989. p. 51–3.

[3] Broadhurts M, Davis GT, McKinney JE. J Appl Phys 1978;49(10):4992–7.

[4] Kepler RG. Ferroelectric, pyroelectric, and piezoelectric properties of poly(vinyliden fluoride). In: Nalwa Hari Singh, editor. Ferroelectric polymers (chemistry, physics, and applications). New York: Marcel Dekker, 1995. p. 183–232.

[5] Tashiro Kohji. Crystal structure and phase transition of PVDF and related copolymers. In: Nalwa Hari Singh, editor. Ferroelectric polymers (chemistry, physics, and applications). New York: Marcel Dekker, 1995. p. 63–181.

[6] Lovinger J. J Polym Sci Polym Phys Ed 1980;18:793–809.

[7] Lovinger J. Science 1983;220:1115–21.

[8] Qudah Ali MA, Al-Raheil Ismail A. Polym Int 1995;38:381–5.

[9] Richardson A, Hope PS, Ward IM. J Polym Sci Polym Phys Ed 1983;21:2525–41.

[10] Sajkiewicz P, Wasiak A, Goclowski Z. Eur Polym J 1999;35:423–9.

[11] Wang YD, Cakmak M. J Appl Polym Sci 1998;68:909–26.

[12] Gregorio Jr R, Cestari M. J Polym Sci Part B Polym Phys 1994;32:859–70.

[13] Matsushige K, Takemura T. J Polym Sci Polym Phys Ed 1978;16:921–34.

[14] Leonard C, Halary JL, Monnerie L, Micheron F. Polym Bull 1984;11:195–202.

[15] El Mohajir B, Heymans N, Companion paper.

[16] Felix Schellekens. Final year project, Université Libre de Bruxelles, 1994.

[17] Bauwens-Crowet C, Bauwens JC. J Mater Sci 1979;14:1817–26.